An Innovative 9-Parameter Magnetic Calibration Method Using Local Magnetic Inclination and Calibrated Acceleration Value

Hairong Yu, Lin Ye, Ying Guo, and Steven Su*

***Abstract*—In this paper, an innovative algorithm for Tri-Axial Magnetometers calibration based on the magnetic inclination is proposed. The proposed "Inclination based Calibration method" uses the fact that the angle between the local gravity and magnetic field is invariant hence overcoming the limitations of most existing in-field calibration methods which require nonlinear optimization. This calibration algorithm is formulated as the solution to a linear least square problem. A commonly used 9-parameter model and its associated 12-observation Icosahedron experimental scheme were developed to evaluate its applicability to calibrated Tri-Axial Magnetometers based on measured acceleration and magnetic data. The results show that the algorithm can provide effective calibration results for the magnetic field in both simulation and experiments. In addition, the influence of accelerometers data applied in this algorithm is investigated by simulation and experiment to demonstrate the importance of accelerometers data accuracy. The acceleration value after effective calibration is demonstrated to make an improvement in the estimation results.**

***Index Terms*—Tri-axial Magnetometers, In-field Calibration, Magnetic Inclination, 9-Parameter.**

I. Introduction

IN the light of the rapid development of Micro Electro Mechanical Systems (MEMS) technology, the chip-based inertial sensors (e.g. Tri-Axial Accelerometers (TAs), Tri-Axial Magnetometers (TMs), Tri-Axial Gyroscopes (TGs), and Inertial Measurement Units (IMUs)) are rapidly improved in terms of size reduction. Nowadays, MEMS accelerometers and magnetometers are widely used in various areas [1]–[5]. The magnetometers measure a constant local magnetic field vector when the magnetic disturbances are not presented. Compared with the accelerometers, the magnetometers are relative with low accuracy as the result of the installation errors, sensor deficiencies and vicinity magnetic interference [6]. To improve the accuracy, the magnetometers need to be calibrated regularly because the errors of the low cost MEMS sensors can be corrupted due to various reasons, such as biases and scale factor deviations, misalignment and nonorthogonality of the sensor axes, sensor fabrication issues and the magnetic deviations induced by the host platform [7], [8]. Hence, regular calibrations are necessary to minimize the interference, such as hard iron and soft iron, to ensure the accuracy of the measurements [2], [9].

Large amounts of auto-calibration methods have recently been developed to calibrate the MEMS and are suitable for the in-field calibration [10]. Several convenient effective in-field calibration methods have been developed, and as mentioned before, the hard iron [7], [11]–[13] and soft iron [2], [8], [9] are eliminated through these calibration methods to minimize interference. The in-field calibration methods can be classified as either "Attitude-Dependent" or "Attitude-Independent" approaches. Compared with "Attitude-Dependent" approaches, the "Attitude-Independent" methods do not require high precision turntables to control the sensor orientation. The parameter estimation of "Attitude-Independent" is commonly based on the nonlinear filtering approaches or nonlinear parameter estimation algorithms [11], [13].

One of the typical "Attitude-Independent" calibration methods focuses on minimizing the difference between the magnitude of the measured magnetic field and that of the local magnetic field [14]. Another "Attitude-Independent" method formulates the calibration problem as an ellipsoid fitting problem [2], [15], [16]. After the ellipsoid fitting calibration, the ellipsoid of data will be mapped to a sphere [6], [17]. These methods are with several advantages and only magnetometers data are needed. However, it is necessary for theses methods to solve a nonlinear estimation problem to identify the coefficients of the tri-axial magnetometers model. Considering these aspects, we intend to develop a new calibration algorithm that combines the acceleration data and magnetic data together for magnetic calibration. The parameter estimation of the proposed method is a simple linear least square algorithm, which can be easily implemented in a wearable device with limited computational power.

The magnetic inclination is the angle between the magnetic field and horizontal plane. The inclination of a magnetic field is a form of useful angle information applied to the 3D space

Hairong Yu is with the Faculty of Engineering and Information Technology, University of Technology Sydney, NSW, 2007, Australia. E-mail: Hairong.Yu@student.uts.edu.au.

Lin Ye is with Intelligent Driving Development Center, Geely Automobile Research Institute Co.,Ltd, Ningbo, Zhejiang, P.R.China, 315336.

Ying Guo is with Data61, The Commonwealth Scientific and Industrial Research Organization, Marsfield, NSW 2122, Australia.

Steven Su* (corresponding author) is with Faculty of Engineering and Information Technology, University of Technology Sydney, NSW, 2007, Australia.

[18]. As the local magnetic inclination is constant, the angle between the local gravity and magnetic field is invariant. The measured accelerometers data together with magnetometers data can be used to estimate the inclination if the sensor is mounted in a static platform or its motion acceleration is much lower than the local gravity [19]. Based on this observation, a so-called Inclination based Calibration method (I-Calibration) is proposed in this paper. For the same location, the inclination is constant and can be found out on the Magnetic-Declination and Inclination Website. The inclination in Sydney (Latitude: $33°52'60''$ S, Longitude: $151°13'0''$ E) is $64°19'$.

In the previous study about TAs and TMs calibration, a 6-parameter model was designed by neglecting three cross-axis sensitivity factors. However, due to the non-orthogonality and misalignment of the tri-axial anisotropic magnetoresistive sensor, as well as the unwanted magnetic interference, the 6-parameter model may not be sufficient to obtain the desired estimation [13], [20], [21]. The 9-parameter auto-calibration model is then adopted to build the I-Calibration algorithm in our work. On the other hand, Design of Experiments (DoE) is vital prior to the calibration to ensure the accuracy and effectiveness of the calibrated results [22]–[25]. The classical DoE theory [26] is applied to generate the experimental schemes for the calibration of TMs in order to improve the quality of the calibration method. The DoE can be achieved by maximizing or minimizing a certain index of the Fisher Information Matrix (FIM), which is related to the classical parameter estimation problem. Several famous design schemes are developed to define the index of FIM, such as G-optimal, D-optimal, E-optimal, ED-optimal, and Ds-optimal design [27]–[29]. In the previous study [21], it has been shown that the 12-observation can potentially reach both G-optimal and D-optimal for 9-parameter TAs or TMs model. Therefore, the 12-observation Icosahedron scheme is adopted to uniformly distribute the experiment points on experimental domains.

In this paper, the proposed novel magnetometers calibration method, 9-parameter I-Calibration, with the 12-observation DoE is developed through simulation and real-time experimentation. This method is based on the fact that the constant inclination can be described by the magnetic field and gravity. The new method can efficiently and reliably estimate the coefficients of the tri-axial magnetometers model by simply using a linear Least Square estimator. As the calibration algorithm requires the acceleration value, it is also necessary to study the effect of calibrated acceleration data on the estimation results compared to the measured acceleration data.

The remainder of this paper is organized as follows. The algorithms are introduced in Section II-A and the simulation is proposed in Section II-B. Section II-C introduces the 12-observation experiment design. The simulation results, experimental results and discussion are presented in Section III. Finally, the conclusion is drawn in Section IV.

II. Method

A. Algorithm for Inclination Based Calibration for Magnetometers

The mathematical model of the tri-axial magnetometers measurements is related to the measurement value $\mathbf{M^m} \in R^3$ and the local magnetic field $\mathbf{M^r} \in R^3$. The model can be expressed as follows:

$$\mathbf{M^r} = \mathbf{G_s}\mathbf{G_e}(\mathbf{M^m} + \mathbf{O}) + \mathbf{n} = \mathbf{G}\mathbf{M^m} + \tilde{\mathbf{O}} + \mathbf{n}, \tag{1}$$

where, matrix $\mathbf{G_s}$ is constructed by scale factors and the matrix $\mathbf{G_e}$ stands for the soft iron causing by the nonorthogonality and misalignment of the tri-axial sensors [7], [21]. The matrix $\mathbf{G} \in R^{3\times3}$ is simplified from $\mathbf{G_s} \times \mathbf{G_e}$ [2], [8], [9]. The offset of measurements is indicated by $\mathbf{O} \in R^3$. The matrix $\tilde{\mathbf{O}} = [\tilde{O}_x \quad \tilde{O}_y \quad \tilde{O}_z]^T$ is the product of $\mathbf{G}$ and $\mathbf{O}$. The Gaussian noise vector with zero mean is presented by $\mathbf{n} = [n_x \quad n_y \quad n_z]^T$.

The distortion matrix $\mathbf{G}$ is expressed as [19] :

$$\mathbf{G} = \begin{bmatrix} G_{xx} & G_{xy} & G_{xz} \\ G_{yx} & G_{yy} & G_{yz} \\ G_{zx} & G_{zy} & G_{zz} \end{bmatrix}. \tag{2}$$

According to the model of local magnetic field and measured value from magnetometers in Eq. (1), the calibrated magnetic value $\mathbf{M^c} = [M_x^c \quad M_y^c \quad M_z^c]^T$ can be calculated by the measured magnetic value $\mathbf{M^m} = [M_x^m \quad M_y^m \quad M_z^m]^T$ with the following formula based on Eq. (1):

$$\begin{cases} M_x^c = G_{xx}M_x^m + G_{xy}M_y^m + G_{xz}M_z^m + \tilde{O}_x \\ M_y^c = G_{yx}M_x^m + G_{yy}M_y^m + G_{yz}M_z^m + \tilde{O}_y \\ M_z^c = G_{zx}M_x^m + G_{zy}M_y^m + G_{zz}M_z^m + \tilde{O}_z. \end{cases} \tag{3}$$

For the purpose of getting the calibrated magnetic value $\mathbf{M^c} \in R^3$, the Inclination based Calibration (I-Calibration) is proposed due to the fact that the local inclination is constant for the same location. In other words, the dot product between the magnetic field $\mathbf{M^r} \in R^3$ and the acceleration field $\mathbf{A^r} \in R^3$ is also constant. Ideally, the inclination angle θ can express the relationship between the real acceleration value $\mathbf{A^r} = [A_x \quad A_y \quad A_z]^T$ and the real magnetic field value $\mathbf{M^r} = [M_x \quad M_y \quad M_z]^T$ [18]:

$$\theta = \frac{\pi}{2} - \cos^{-1}\left(\frac{A_xM_x + A_yM_y + A_zM_z}{\|\mathbf{A^r}\|\|\mathbf{M^r}\|}\right). \tag{4}$$

As mentioned before, the dot product between the local magnetic field $\mathbf{M^r} \in R^3$ and the gravity field $\mathbf{A^r} \in R^3$ is invariant, a constant L can be defined to express the relationship between $\mathbf{A^r}$ and $\mathbf{M^r}$ in Eq. (4):

$$\mathrm{L} = A_xM_x + A_yM_y + A_zM_z = \|\mathbf{A^r}\|\|\mathbf{M^r}\|\cos\left(\frac{\pi}{2} - \theta\right). \tag{5}$$

In order to formulate the 9-parameter model for Eq. (3), we assume $G_{yx} = G_{xy}$, $G_{zx} = G_{xz}$, $G_{zy} = G_{yz}$. The unknown parameter matrix $\boldsymbol{\beta}$ for 9-parameter I-Calibration algorithm can be expressed as:

This article has been accepted for publication in a future issue of this journal, but has not been fully edited. Content may change prior to final publication. Citation information: DOI 10.1109/JSEN.2020.2995876, IEEE Sensors Journal

$$\boldsymbol{\beta} = [G_{xx} \quad \tilde{O}_x \quad G_{yy} \quad \tilde{O}_y \quad G_{zz} \quad \tilde{O}_z \quad G_{xy} \quad G_{xz} \quad G_{yz}]^T. \quad (6)$$

To ensure the accuracy of the magnetic calibration results, the measured acceleration value $\mathbf{A^m} = [A_x^m \quad A_y^m \quad A_z^m]^T$ is first calibrated by the approach which proposed in our previous work [30] and identified as $\mathbf{A^c} = [A_x^c \quad A_y^c \quad A_z^c]^T$. Based on Eq. (5) and Eq. (3), the calibration formula which expresses the relationship between the measured magnetic value $\mathbf{M^m} = [M_x^m \quad M_y^m \quad M_z^m]^T$, the calibrated acceleration value $\mathbf{A^c} = [A_x^c \quad A_y^c \quad A_z^c]^T$ and the constant L is expanded as:

$$\begin{aligned} \mathrm{L} &= A_x^c M_x^c + A_y^c M_y^c + A_z^c M_z^c \\ &= A_x^c(G_{xx}M_x^m + G_{xy}M_y^m + G_{xz}M_z^m + \tilde{O}_x) \\ &+ A_y^c(G_{yx}M_x^m + G_{yy}M_y^m + G_{yz}M_z^m + \tilde{O}_y) \\ &+ A_z^c(G_{zx}M_x^m + G_{zy}M_y^m + G_{zz}M_z^m + \tilde{O}_z). \end{aligned} \quad (7)$$

Eq. (7) can be stacked to a matrix form as shown in Eq. (8) (See next page) when there are n sets of measurement data and $\boldsymbol{\varepsilon} \in R^n$ is the measurement noise.

The constant L can be calculated by the local inclination θ based on Eq. (4) and Eq. (5) and simply written as follows based on Eq. (7):

$$\mathbf{L} = \mathbf{X}\boldsymbol{\beta} + \boldsymbol{\varepsilon}, \quad (9)$$

where

$$\mathbf{X} = \begin{bmatrix} A_{x1}^c M_{x1}^m & \cdots & \cdots & A_{xn}^c M_{xn}^m \\ A_{x1}^c & \cdots & \cdots & A_{xn}^c \\ A_{y1}^c M_{y1}^m & \cdots & \cdots & A_{yn}^c M_{yn}^m \\ A_{y1}^c & \cdots & \cdots & A_{yn}^c \\ A_{z1}^c M_{z1}^m & \cdots & \cdots & A_{zn}^c M_{zn}^m \\ A_{z1}^c & \cdots & \cdots & A_{zn}^c \\ A_{x1}^c M_{y1}^m + A_{y1}^c M_{x1}^m & \cdots & \cdots & A_{xn}^c M_{yn}^m + A_{yn}^c M_{xn}^m \\ A_{x1}^c M_{z1}^m + A_{z1}^c M_{x1}^m & \cdots & \cdots & A_{xn}^c M_{zn}^m + A_{zn}^c M_{xn}^m \\ A_{y1}^c M_{z1}^m + A_{z1}^c M_{y1}^m & \cdots & \cdots & A_{yn}^c M_{zn}^m + A_{zn}^c M_{yn}^m \end{bmatrix}^T. \quad (10)$$

Then, a least square estimation problem can be formulated to calculate the parameters $\boldsymbol{\beta}$ in Eq.(9):

$$\hat{\boldsymbol{\beta}} = (\mathbf{X}^{\mathrm{T}}\mathbf{X})^{-1}\mathbf{X}^{\mathrm{T}}\mathbf{L}. \quad (11)$$

After the parameters $\boldsymbol{\beta}$ is calculated, the calibrated magnetic value $\mathbf{M^c} = [M_x^c \quad M_y^c \quad M_z^c]^T$ value by I-Calibration is calculated according to Eq. (3) and Eq. (6).

B. Simulation Study

As the calibration algorithm utilizes the local gravity information, which is measured by TAs, the overall performance of the proposed calibration method is influenced by the estimated gravity. For the purpose of studying the influence of accelerometers value accuracy on the calibration results and evaluating the I-Calibration approach, the simulation study is developed. Firstly, the simulated TAs output value $\mathbf{A^s} \in R^3$ is generated according to the theoretical projection of the earth's gravity, and deliberately added errors to the model parameters. Specifically, the scale factors are set within $\pm 10\%$ and offsets are within $\pm 0.1g$ [30]. In order to implement the angle between the gravity and magnetic field during simulation, the simulated TMs value $\mathbf{M^s}$ is generated as the projection of acceleration value $\mathbf{A^s}$ in the magnetic axis according to the inclination angle θ. To make a comparison, before calibration, we assume there are additional errors of scale factors $\pm 10\%$ and offset within $\pm 0.1g$ in the TAs model, and use $\mathbf{A_n^s}$ to stand for the uncalibrated TAs output. Then, the 12-observation DoE is adopted to acquire the observation matrix $\mathbf{X}$ as introduced in Section II-A after the simulated data have been generated. At last, $\mathbf{A^s}$ and $\mathbf{M^s}$, $\mathbf{A_n^s}$ and $\mathbf{M^s}$ are substituted in the formula of I-Calibration method respectively to obtain the simulation calibration results.

C. Experimental Design

The experiment was performed by using the commercially IMU device (VICON IMeasureU, Auckland, New Zealand). The IMU sensor, the interface of mobile phone application (APP) and desktop software are shown in Fig.1 (a). The experiment was implemented at the campus of the University of Technology Sydney and was performed far away from magnetic materials to ensure a homogeneous local magnetic field. This aims to discard perturbation from the hosting platform to measure the earth's field. Meanwhile, as the experiment is performed in clean ferromagnetic surroundings, the measured value from magnetometers can be approximately equal to the local magnetic field. As mentioned previously, we adopt the 12-observation scheme [13] to calibrate the magnetometers. During the experiment, the IMU sensor was rotated to 12 positions with respect to the local horizontal frame, and was placed in each position according to the 12-observation in Fig.1 (b) for a certain period to record steady data. The x, y, z in Fig.1 (b) indicate the positive direction in each axis. The data can be stored for further processing after the 12-observation experiment completed. This calibration procedure can be repeated to reduce the influence of sensor drift [24].

III. Results and Discussion

A. Simulation for Inclination based Calibration

The sum of the square of the magnetic data is magnitude, which is a vital factor to interpret the effectiveness of calibration [31], [32]. A randomly selected example of the simulation results is presented in Fig. 2 which shows the scaled magnitude value of magnetic field before and after the I-Calibration simulation. The calibration results calculated by the measured (raw) acceleration value and calibrated acceleration value are represented respectively.

According to the magnitude of the magnetic field after 2000 times I-Calibration simulation with different measured and

This article has been accepted for publication in a future issue of this journal, but has not been fully edited. Content may change prior to final publication. Citation information: DOI 10.1109/JSEN.2020.2995876, IEEE Sensors Journal

$$\begin{bmatrix} A_{x1}^c M_{x1}^m & A_{x1}^c & A_{y1}^c M_{y1}^m & A_{y1}^c & A_{z1}^c M_{z1}^m & A_{z1}^c & A_{x1}^c M_{y1}^m + A_{y1}^c M_{x1}^m & A_{x1}^c M_{z1}^m + A_{z1}^c M_{x1}^m & A_{y1}^c M_{z1}^m + A_{z1}^c M_{y1}^m \\ \cdots & \cdots & \cdots & \cdots & \cdots & \cdots & \cdots & \cdots & \cdots \\ \vdots & \vdots & \vdots & \vdots & \vdots & \vdots & \vdots & \vdots & \vdots \\ \vdots & \vdots & \vdots & \vdots & \vdots & \vdots & \vdots & \vdots & \vdots \\ A_{xn}^c M_{xn}^m & A_{xn}^c & A_{yn}^c M_{yn}^m & A_{yn}^c & A_{zn}^c M_{zn}^m & A_{zn}^c & A_{xn}^c M_{yn}^m + A_{yn}^c M_{xn}^m & A_{xn}^c M_{zn}^m + A_{zn}^c M_{xn}^m & A_{yn}^c M_{zn}^m + A_{zn}^c M_{yn}^m \end{bmatrix} \begin{bmatrix} G_{xx} \\ \tilde{O}_x \\ G_{yy} \\ \tilde{O}_y \\ G_{zz} \\ \tilde{O}_z \\ G_z \\ G_{xy} \\ G_{xz} \\ G_{yz} \end{bmatrix} + \boldsymbol{\varepsilon} = \begin{bmatrix} L \\ \cdots \\ L \end{bmatrix}. \tag{8}$$

(a) The IMU Device, Interface of Application and Software used in Experiment.

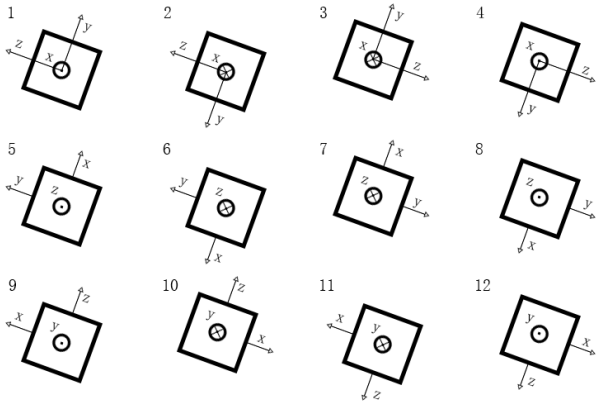

(b) The Arrangements of MEMS IMU for 12-Observation DoE.

Fig. 1. The Experimental Device, Interface and 12-Observation DoE.

calibrated acceleration values, the range and standard deviation of magnitude are calculated and represented in Fig. 3.

From the above results, it is demonstrated that the I-Calibration is an effective magnetic calibration method as the magnitude of the magnetic field is more accurate after calibration. In addition, the acceleration data after calibration is helpful to improve the magnetic calibration results.

B. Experimental Results for Inclination based Calibration

The magnitudes of the calibrated magnetometers data $\mathbf{M^c}$ and the measured magnetometers data $\mathbf{M^m}$ are also applied as indicators to demonstrate the effectiveness of calibration in the experiment. The scaled magnitude of the calibrated magnetometers data can be seen to lie around 1 as depicted in yellow in Fig. 4.

As mentioned in Section II-A, the acceleration value has been calibrated when the I-Calibration is applied to the magnetic calibration. In order to illustrate the influence of acceleration value accuracy on the calibration results, a contrast is proposed by implementing the measured acceleration value $\mathbf{A^m} = [A_x^m \quad A_y^m \quad A_z^m]^T$ without calibration in Eq. (7). The scaled magnitude before and after I-Calibration by using uncalibrated acceleration value is shown in red in Fig. 4.

Generally, if the magnetic distortion and sensor error exist, the magnetometers data without calibration will lie on an ellipsoid surface. Once the magnetic value has been calibrated properly, this data will be distributed in a unit sphere [8], [19], [33]. In order to display the raw data, the calibrated magnetic data by I-Calibration using measured acceleration value $\mathbf{A^m}$ and using calibrated acceleration value $\mathbf{A^c}$ directly, Fig. 5 is presented to make a contrast for them with a sphere reference plane.

Notation H_0 represents the magnitude of raw magnetic data, while H_1 and H_2 stand for the magnitudes of calibrated magnetic data by I-Calibration with measured and calibrated accelerations, respectively. In Table I, the range (the difference

This article has been accepted for publication in a future issue of this journal, but has not been fully edited. Content may change prior to final publication. Citation information: DOI 10.1109/JSEN.2020.2995876, IEEE Sensors Journal

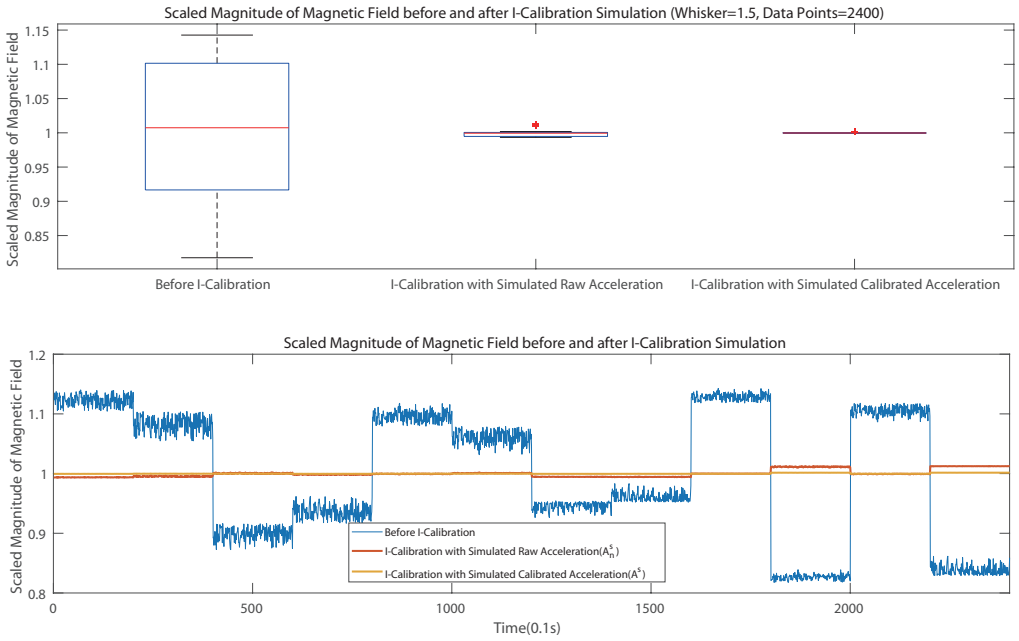

Fig. 2. Scaled Magnitude (around 1) of Raw and Calibrated Data by I-Calibration Simulation with Measured Acceleration and Calibrated Acceleration Data.

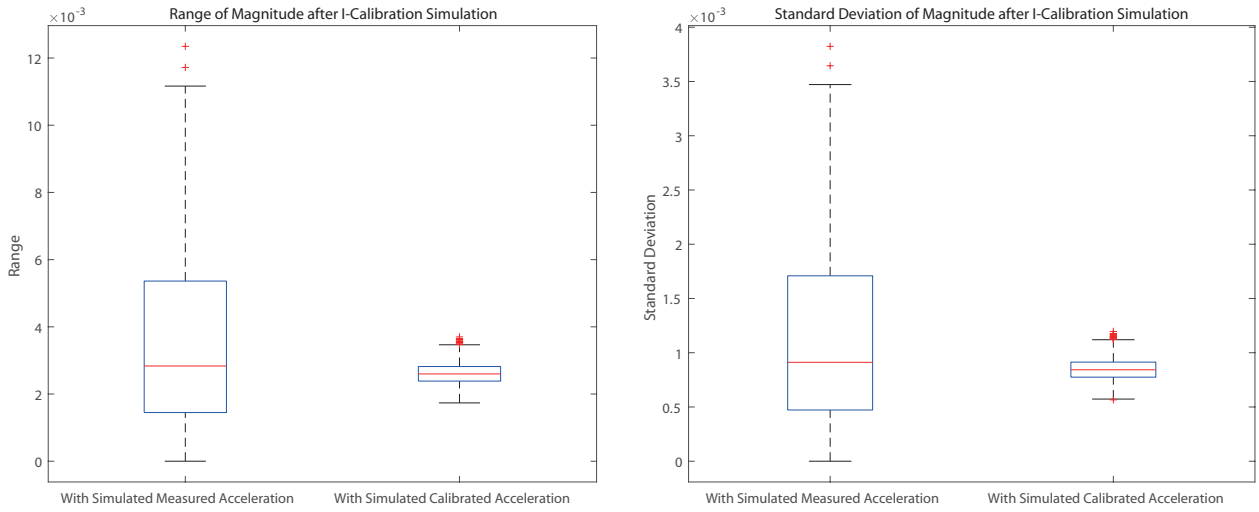

Fig. 3. Range and Standard Deviation of Magnitude after I-Calibration Simulation with Measured Acceleration Data and Calibrated Acceleration Data (Whisker=1.5, Repeat times=2000).

between the largest and smallest values of the magnitudes) indicates the measures of variation and the standard deviation (SD) represents the dispersion of H_0, H_1 and H_2. In addition, the mean absolute deviation (MAD) and mean absolute value (MAV) are listed in Table I to demonstrate the deviation of H_1 and H_2 from the baseline, which is defined as 1. Moreover, the errors between the baseline and H_0, H_1, H_2 are displayed in Fig. 6.

The improvement comparisons for the magnetic calibration by the I-Calibration method and the importance of the accel-

TABLE I
THE COMPARISONS FOR MAGNITUDE OF RAW DATA AND CALIBRATED DATA BY I-CALIBRATION WITH CALIBRATED ACCELERATION $\mathbf{A^c}$ AND MEASURED ACCELERATION $\mathbf{A^m}$.

Method	H_0	H_1	H_2
Range	0.4699	0.1694	0.0953
SD	0.1186	0.0282	0.0142
MAD	/	0.0206	0.0098
MAV	/	0.0299	0.0115

This article has been accepted for publication in a future issue of this journal, but has not been fully edited. Content may change prior to final publication. Citation information: DOI 10.1109/JSEN.2020.2995876, IEEE Sensors Journal

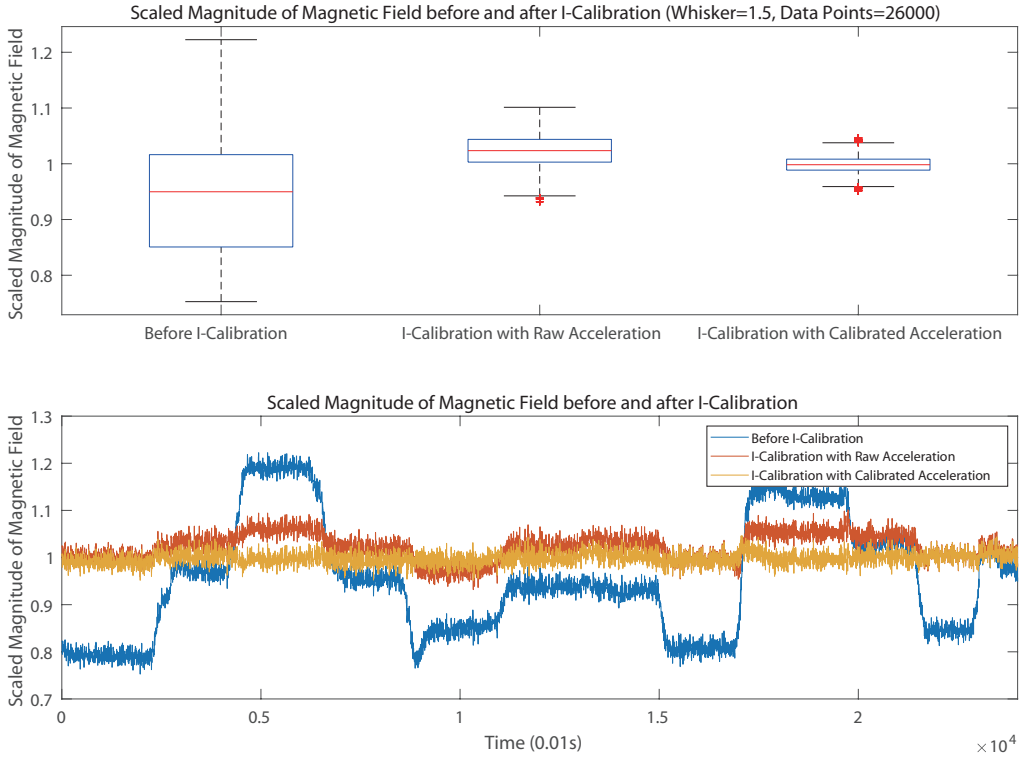

Fig. 4. Scaled Magnitude (around 1) Value before and after I-Calibration with Calibrated Acceleration $\mathbf{A^c}$ and Measured Acceleration $\mathbf{A^m}$.

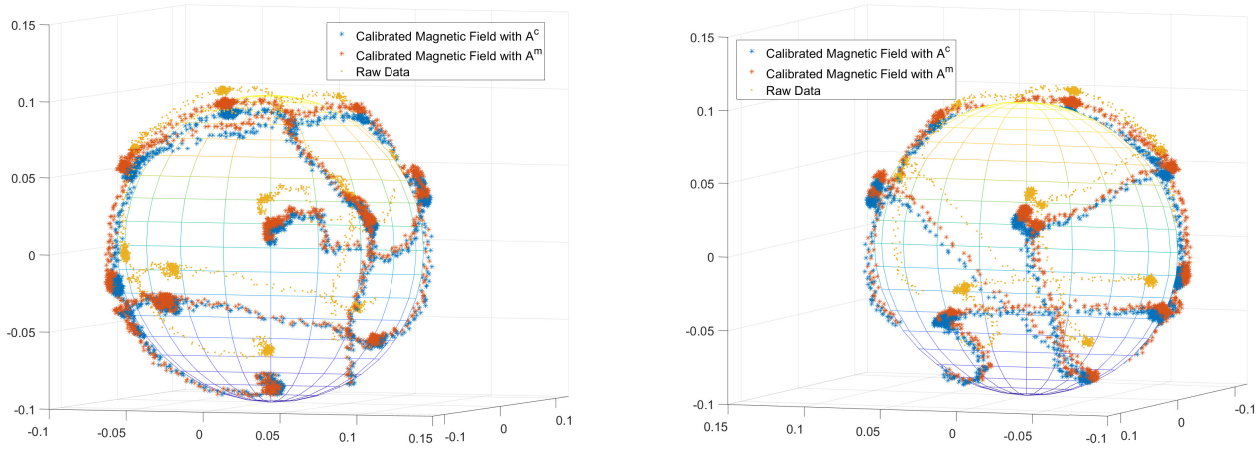

(a) Front View (b) Back View

Fig. 5. Raw Data and Calibrated Data by I-Calibration with Calibrated Acceleration $\mathbf{A^c}$ and Measured Acceleration $\mathbf{A^m}$

eration data calibration are listed in Table II according to the statistical indicators in Table I.

The experimental results lead to the same conclusion with the simulation that the I-Calibration is effective on magnetic calibration and the acceleration data should be calibrated to ensure accurate calibration results.

TABLE II
THE IMPROVEMENT COMPARISONS FOR THE STATISTICAL INDICATORS.

Comparison	H_1 *to* H_0	H_2 *to* H_0	H_2 *to* H_1
Range	63.94%	79.72%	43.76%
SD	76.20%	87.98%	49.50%
MAD	/	/	52.18%
MAV	/	/	61.44%

This article has been accepted for publication in a future issue of this journal, but has not been fully edited. Content may change prior to final publication. Citation information: DOI 10.1109/JSEN.2020.2995876, IEEE Sensors Journal

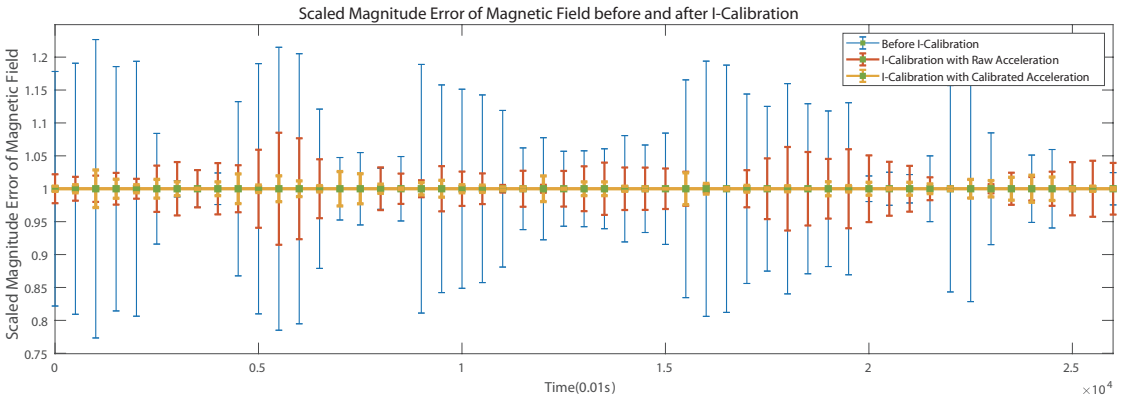

Fig. 6. Scaled Magnitude (around 1) Error before and after I-Calibration with Calibrated Acceleration $\mathbf{A^c}$ and Measured Acceleration $\mathbf{A^m}$.

C. Discussion

The proposed I-Calibration method in this paper is demonstrated to be effective in calibrating the magnetometers both by simulation and experiment. The measured magnetic field data and calibrated acceleration data has been applied to both simulation and experiment magnetometers calibrations. From the results shown in Fig. 4, the scaled magnitude of the calibrated magnetometers data can be seen to lie around 1 which means the data have been calibrated effectively [31]–[33]. The results in Fig. 5 also displays that the data is mapped to a sphere after calibration [8], [19], [33].

For the purpose of demonstrating whether the acceleration data has an influence on the I-Calibration method, the simulation and experimental calibration have also been implemented by the raw acceleration data. It can be noticed that when the acceleration data is without calibration, the scaled magnitude of the magnetic field is with deviation from the baseline of 1 in Fig. 2 and Fig. 4. The deviation is proved by the decreased range and standard deviation of the magnetic field magnitude after the I-Calibration simulation in Fig. 3. The calibrated TMs data with raw acceleration data as shown in Fig. 5 are also with deviation from the reference sphere. The percentage of the improvement for the magnetic calibration results when the acceleration data is calibrated is displayed in Table I and provides the statistical evidence for the deviation. As we can see, both the range and the standard deviation of the magnitude of the magnetic field is decreased after calibration, and the extent of decreasing when using calibrated acceleration is larger compared to that which use the measured acceleration. The decreased MAD and MAV by different acceleration values also illustrate the necessity of acceleration calibration. According to the results both from simulation and experiment, the improvement in the calibration results when using the calibrated acceleration data is demonstrated.

Above all, compared to the existing "Attitude-Independent" calibration methods which need some extra conditions to ensure the convergence of the algorithm [30], [34] (as it is a nonlinear parameter estimation algorithm and needs appropriate selected initial conditions [19], [33]), the proposed I-Calibration is a simple linear method, i.e., it is a single step linear least square estimator without iteration. Thus, the method can be easily implemented in a wearable device with low computational power. However, the performance of tri-axial accelerometers is essential to ensure the success of the proposed I-Calibration method as the uncalibrated accelerometers data can affect the calibration results as shown in Section III.

IV. Conclusion

A practical algorithm named Inclination based Calibration is developed to calibrate the Tri-Axial Magnetometers. This algorithm is based on the fact that the angle between the local magnetic field and gravity is constant. A 9-parameter mathematical method associated with the 12-observation experimental design is proposed for the calibration procedure. The problem is finally formulated as a linear least square problem based on the measured magnetic value and calibrated acceleration value. The algorithm performs well on both the simulation study and practical experiment. To investigate the significance of the accuracy of the acceleration value, a contrast study is applied in the simulation and experimental procedure. It demonstrates that the acceleration data should be calibrated well to ensure the effectiveness of the Inclination based Calibration algorithm.

Limitations

Firstly, according to the conclusion, as the calibration accuracy of the proposed I-Calibration method is affected by the tri-axial accelerometers, it is recommended to perform a calibration for the tri-axial accelerometers before using I-Calibration. Secondly, the exact value of inclination in different locations may vary with time. However, as long as the L maintains a constant value during the calibration, the validity of the calibration could be guaranteed. Thirdly, the experiments should be performed in a similar location for each calibration.

REFERENCES

[1] H. Schmidt, N. R. Rypkema, and E. Fischell, "Submerged vehicle localization system and method," Jul. 4 2019, uS Patent App. 16/237,463.

[2] V. Renaudin, M. H. Afzal, and G. Lachapelle, "Complete triaxis magnetometer calibration in the magnetic domain," *Journal of sensors*, vol. 2010, 2010.

[3] A. K. Bourke, P. Van De Ven, M. Gamble, R. O'Connor, K. Murphy, E. Bogan, E. McQuade, P. Finucane, G. ÓLaighin, and J. Nelson, "Assessment of waist-worn tri-axial accelerometer based fall-detection algorithms using continuous unsupervised activities," in *2010 Annual International Conference of the IEEE Engineering in Medicine and Biology*. IEEE, 2010, pp. 2782–2785.

[4] T. Lei, A. A. Mohamed, and C. Claudel, "An imu-based traffic and road condition monitoring system," *HardwareX*, vol. 4, p. e00045, 2018.

[5] M. H. Afzal, V. Renaudin, and G. Lachapelle, "Assessment of indoor magnetic field anomalies using multiple magnetometers," in *ION GNSS*, vol. 10, 2010, pp. 21–24.

[6] D. Gebre-Egziabher, G. H. Elkaim, J. David Powell, and B. W. Parkinson, "Calibration of strapdown magnetometers in magnetic field domain," *Journal of Aerospace Engineering*, vol. 19, no. 2, pp. 87–102, 2006.

[7] J. Fang, H. Sun, J. Cao, X. Zhang, and Y. Tao, "A novel calibration method of magnetic compass based on ellipsoid fitting," *IEEE Transactions on Instrumentation and Measurement*, vol. 60, no. 6, pp. 2053–2061, 2011.

[8] V. Renaudin, M. H. Afzal, and G. Lachapelle, "New method for magnetometers based orientation estimation," in *IEEE/ION Position, Location and Navigation Symposium*. IEEE, 2010, pp. 348–356.

[9] P. Guo, H. Qiu, Y. Yang, and Z. Ren, "The soft iron and hard iron calibration method using extended kalman filter for attitude and heading reference system," in *2008 IEEE/ION Position, Location and Navigation Symposium*. IEEE, 2008, pp. 1167–1174.

[10] M. Glueck, D. Oshinubi, P. Schopp, and Y. Manoli, "Real-time autocalibration of mems accelerometers," *IEEE Transactions on Instrumentation and Measurement*, vol. 63, no. 1, pp. 96–105, 2013.

[11] J. L. Crassidis, K.-L. Lai, and R. R. Harman, "Real-time attitude-independent three-axis magnetometer calibration," *Journal of Guidance, Control, and Dynamics*, vol. 28, no. 1, pp. 115–120, 2005.

[12] W. Koo, S. Sung, and Y. J. Lee, "Error calibration of magnetometer using nonlinear integrated filter model with inertial sensors," *IEEE Transactions on Magnetics*, vol. 45, no. 6, pp. 2740–2743, 2009.

[13] L. Ye and S. W. Su, "Optimum experimental design applied to mems accelerometer calibration for 9-parameter auto-calibration model," in *2015 37th Annual International Conference of the IEEE Engineering in Medicine and Biology Society (EMBC)*. IEEE, 2015, pp. 3145–3148.

[14] R. Alonso and M. D. Shuster, "Complete linear attitude-independent magnetometer calibration," *Journal of the Astronautical Sciences*, vol. 50, no. 4, pp. 477–490, 2002.

[15] I. Markovsky, A. Kukush, and S. Van Huffel, "Consistent least squares fitting of ellipsoids," *Numerische Mathematik*, vol. 98, no. 1, pp. 177–194, 2004.

[16] J. F. Vasconcelos, G. Elkaim, C. Silvestre, P. Oliveira, and B. Cardeira, "Geometric approach to strapdown magnetometer calibration in sensor frame," *IEEE Transactions on Aerospace and Electronic systems*, vol. 47, no. 2, pp. 1293–1306, 2011.

[17] W. Gander, G. H. Golub, and R. Strebel, "Least-squares fitting of circles and ellipses," *BIT Numerical Mathematics*, vol. 34, no. 4, pp. 558–578, 1994.

[18] D. Y. Kim, B. K. Kim, S. H. Park, K. S. KI, H. S. Shin, J. A. Na, Y. J. Kim, and Y. S. Choi, "Method for calculating the angle of inclination of magnetic field in a sensor coordination system," Mar. 2 2017, uS Patent App. 15/132,545.

[19] M. Kok, J. D. Hol, T. B. Schön, F. Gustafsson, and H. Luinge, "Calibration of a magnetometer in combination with inertial sensors," in *2012 15th International Conference on Information Fusion*. IEEE, 2012, pp. 787–793.

[20] S.-h. P. Won and F. Golnaraghi, "A triaxial accelerometer calibration method using a mathematical model," *IEEE Transactions on Instrumentation and Measurement*, vol. 59, no. 8, pp. 2144–2153, 2009.

[21] L. Ye and S. W. Su, "Experimental design for the calibration of triaxial magnetometers," in *2015 9th International Conference on Sensing Technology (ICST)*. IEEE, 2015, pp. 711–715.

[22] R. S. Methodology, "Process and product optimization using designed experiments," *Myers, RH and Montgomery, DC, John Wiely & Sons, New York*, 1995.

[23] A. Atkinson, A. Donev, and R. Tobias, *Optimum experimental designs, with SAS*. Oxford University Press, 2007, vol. 34.

[24] R. H. Myers, D. C. Montgomery, and C. M. Anderson-Cook, *Response surface methodology: process and product optimization using designed experiments*. John Wiley & Sons, 2016.

[25] D. C. Montgomery, *Design and analysis of experiments*. John wiley & sons, 2017.

[26] A. I. Khuri and S. Mukhopadhyay, "Response surface methodology," *Wiley Interdisciplinary Reviews: Computational Statistics*, vol. 2, no. 2, pp. 128–149, 2010.

[27] R. Mehra, "Optimal input signals for parameter estimation in dynamic systems–survey and new results," *IEEE Transactions on Automatic Control*, vol. 19, no. 6, pp. 753–768, 1974.

[28] S. Asprey and S. Macchietto, "Designing robust optimal dynamic experiments," *Journal of Process Control*, vol. 12, no. 4, pp. 545–556, 2002.

[29] M. Patan and D. UcińSki, "Configuring a sensor network for fault detection in distributed parameter systems," *International Journal of Applied Mathematics and Computer Science*, vol. 18, no. 4, pp. 513–524, 2008.

[30] L. Ye, Y. Guo, and S. W. Su, "An efficient autocalibration method for triaxial accelerometer," *IEEE Transactions on Instrumentation and Measurement*, vol. 66, no. 9, pp. 2380–2390, 2017.

[31] C. C. Foster and G. H. Elkaim, "Extension of a two-step calibration methodology to include nonorthogonal sensor axes," *IEEE Transactions on Aerospace and Electronic Systems*, vol. 44, no. 3, pp. 1070–1078, 2008.

[32] J. C. Springmann and J. W. Cutler, "Attitude-independent magnetometer calibration with time-varying bias," *Journal of Guidance, Control, and Dynamics*, vol. 35, no. 4, pp. 1080–1088, 2012.

[33] M. Kok and T. B. Schön, "Magnetometer calibration using inertial sensors," *IEEE Sensors Journal*, vol. 16, no. 14, pp. 5679–5689, 2016.

[34] I. Frosio, F. Pedersini, and N. A. Borghese, "Autocalibration of mems accelerometers," *IEEE Transactions on Instrumentation and Measurement*, vol. 58, no. 6, pp. 2034–2041, 2008.

Hairong Yu received the B.E. degree in biomedical engineering from the Sun-Yat Sen University, Guangzhou, China, in 2016. She is currently a Ph.D. student at University of Technology Sydney in Australia. Her current research interests are system modelling, biomedical signal processing and calibration for wearable devices and sensors.

Lin Ye received the B.E. (Hons. I) degree in electrical engineering from the University of Technology Sydney, Sydney, Australia, in 2013 and received the Ph.D. degree with the Center for Health Technologies in 2018. His current research interests include system identification, modeling of cardiorespiratory response, and calibration of inertial measurement unit.

Ying Guo received the B.E. and M.E. degrees from Northwestern Polytechnic University, Xi'an, China, in 1994 and 1995, respectively, and the Ph.D. degree in machine learning from Australian National University, Canberra, ACT, Australia, in 2001. She is currently a Senior Research Scientist with the CSIRO Data61, Marsfield, NSW 2122. Her current research interests include machine learning, intelligent sensor networks, pattern recognition, and fault diagnostic.

Steven Su received the B.S. and M.S. degrees from the Harbin Institute of Technology, Harbin, China, in 1990 and 1993, respectively, and the Ph.D. degree from the Research School of Information Sciences and Engineering, Australian National University, Canberra, ACT, Australia, in 2002. He was a Post-Doctoral Research Fellow with the Faculty of Engineering, University of New South Wales, Sydney, NSW, Australia, from 2002 to 2006. He is currently an Associate Professor with the Faculty of Engineering and IT, University of Technology Sydney, Sydney. His current research interests include biomedical system modeling and control, robust and adaptive control, fault tolerant control, and wearable monitoring system.